

Available online at www.sciencedirect.com

ScienceDirect

journal homepage: www.elsevier.com/locate/bbe

Original Research Article

Segmentation of brain MR images using rough set based intuitionistic fuzzy clustering

Yogita K. Dubey^{a,*}, Miind M. Mushrif^a, Kajal Mitra^b

^aDepartment of Electronics & Telecommunication, Yeshwantrao Chavan College of Engineering, Nagpur 441 110, Maharashtra, India

^bDepartment of Radio-diagnosis and Imaging Center, NKP Salve Institute of Medical Sciences and Lata Mangeshkar Hospital, Nagpur, India

ARTICLE INFO

Article history:

Received 2 September 2015

Received in revised form

27 November 2015

Accepted 6 January 2016

Available online xxx

Keywords:

Segmentation

Magnetic resonance

Brain image

Rough set

Intuitionistic fuzzy set

Fuzzy c-means clustering

ABSTRACT

Intuitionistic fuzzy sets and rough sets are widely used for medical image segmentation, and recently combined together to deal with uncertainty and vagueness in medical images. In this paper, a rough set based intuitionistic fuzzy c-means (RIFCM) clustering algorithm is proposed for segmentation of the magnetic resonance (MR) brain images. Firstly, we proposed a new automated method to determine the initial values of cluster centroid using intuitionistic fuzzy roughness measure, obtained by considering intuitionistic fuzzy histogram as upper approximation of rough set and fuzzy histogram as lower approximation of rough set. A new intuitionistic fuzzy complement function is proposed for intuitionistic fuzzy image representation to take into account intensity inhomogeneity and noise in brain MR images. The results of segmentation of proposed algorithm are compared with the existing rough set based fuzzy clustering algorithms, intuitionistic fuzzy clustering and bias corrected fuzzy clustering algorithm. Experimental results demonstrate the superiority of proposed algorithm.

© 2016 Nałęcz Institute of Biocybernetics and Biomedical Engineering of the Polish Academy of Sciences. Published by Elsevier Sp. z o.o. All rights reserved.

1. Introduction

Study of brain function and brain disorder requires accurate segmentation of magnetic resonance (MR) brain images into three main tissue types: cerebro spinal fluid (CSF), gray matter (GM) and white matter (WM). Manual delineation of these brain tissues by a human expert is time consuming and

induces large intra and inter-observer variability because of intensity inhomogeneity and noise in images.

Fuzzy c-means clustering (FCM) is widely used for image segmentation. But FCM clustering fails to deal with local spatial property of images which leads to strong noise sensibility. Since medical images always include considerable uncertainty and unknown noise, this generally leads to degradation in segmentation quality.

* Corresponding author at: Department of Electronics and Telecommunication, Yeshwantrao Chavan College of Engineering, Nagpur 441 110, Maharashtra, India.

E-mail addresses: yogeetadubey@yahoo.co.in (Y.K. Dubey), milindmushrif@yahoo.com (M.M. Mushrif), kajalmitra@gmail.com (K. Mitra).

<http://dx.doi.org/10.1016/j.bbe.2016.01.001>

0208-5216/© 2016 Nałęcz Institute of Biocybernetics and Biomedical Engineering of the Polish Academy of Sciences. Published by Elsevier Sp. z o.o. All rights reserved.

Many algorithms [1-3] are proposed to overcome the problems related to FCM. In these algorithms, spatial information is incorporated in objective function of original FCM to improve the performance of image segmentation.

Bias corrected fuzzy c-means clustering (FCM) algorithm [4], spatially constrained kernelized FCM algorithms [5], improved fuzzy segmentation algorithm [6], fast generalized FCM [7], Gaussian kernel based FCM algorithm [8], and FCM based multi-scale diffusion filtering scheme [9] are proposed for brain image segmentation. All these methods are found to be affected by their parameters selection and lack of robustness to noise.

Multilevel methods [10,11], model based approaches [12-16] and level set approaches [17,18] are also used for brain image segmentation and tumor detection. Recently, histon based thresholding methods are used for image segmentation. The concept of histon was originally proposed by Mohabey and Ray [19]. The segmentation algorithm proposed by Mohabey and Ray [19] does not take into account the lower approximation and thus fails to utilize the properties of the boundary region between the two approximations in segmentation. Mushrif and Ray [20] proposed a color image segmentation method that uses roughness index for segmentation. Miao et al. [21] proposed multiscale roughness measure for segmentation of color images.

Intuitionistic fuzzy set (IFS) approaches are also being used for image segmentation. Since IFS takes into accounts non-membership and hesitancy value along with membership value, these sets are useful to deal with uncertainty and vagueness in the pixel intensities of the images. Mushrif and Ray [22] proposed intuitionistic fuzzy roughness index based color image segmentation method. Intuitionistic fuzzy set based c means clustering approach is used for the segmentation of medical images in [23-25]. But FCM based clustering methods are dependent on parameter selection, sensitive to noise and their convergence mainly depends on initialization of cluster centroid. These limitations may cause the algorithm to get stuck in a local optimum which may reduce the segmentation accuracy.

In this work, rough set based intuitionistic fuzzy clustering algorithm is proposed for the segmentation of brain MR images. The main contributions of present work are:

1. Intuitionistic fuzzy image representation is used using proposed fuzzy complement function to take into account intensity inhomogeneity and noise in brain MR images.
2. Intuitionistic fuzzy roughness measure is calculated by considering fuzzy histogram as lower approximation and intuitionistic fuzzy histon as upper approximation of rough set.
3. Cluster centroid for intuitionistic FCM clustering is initialized by peak points of intuitionistic fuzzy roughness measure.
4. Intuitionistic FCM clustering is performed using intuitionistic fuzzy image representation incorporating membership, non-membership and hesitation index.
5. Cluster centroid and membership matrix of intuitionistic FCM clustering are updated using intuitionistic fuzzy similarity measure.
6. The proposed algorithm segments synthetic brain MR image into three regions, gray matter (GM), white matter

(WM) and cerebro-spinal fluid (CSF) and separates edema, cysts components and tumor tissues in real brain images. The new algorithm improves the conventional FCM clustering process by reducing the randomness in the initialization of cluster centroid. The algorithm uses intuitionistic fuzzy representation of image to deal with variations in pixel intensities of brain MR images. A new intuitionistic fuzzy complement function is proposed to find the hesitancy in an image which works better than Sugeno [26] and Yagers [27] fuzzy complement. The proposed rough set based intuitionistic fuzzy clustering algorithm segments brain MR image into three regions, cerebro-spinal fluid, gray matter and white matter, which is very useful for the diagnosis of degenerative brain diseases.

The rest of the paper is organized as follows: preliminary concepts are described in Section 2, Section 3 describes the proposed algorithm, experimental results are given in Section 4, followed by the conclusion in Section 5.

2. Preliminary concepts

In this section, we present the preliminary concepts of rough set theory and intuitionistic fuzzy set theory.

2.1. Rough Set

According to the definition given by Pawlak [28], an information system is a pair $S = \langle U, A, V, f \rangle$ or a function $f: U \times A \rightarrow V$, where U is nonempty finite set of N objects $\{x_1, x_2, \dots, x_N\}$ called the universe, A is a non-empty finite set of attributes, and V is value set such that $a: U \rightarrow V_a$ for every $a \in A$. The set V_a is the set of values of attribute a , called the domain of a . Given any subset of attributes B , any concept $X \subseteq U$ can be defined approximately by employing two exact sets called lower approximation $\underline{BX} = \cup \{Y \in U | IND(B) : Y \subseteq X\}$ and upper approximation $\overline{BX} = \cup \{Y \in U | IND(B) : Y \cap X \neq \emptyset\}$. The set \underline{BX} is the set of all elements of U which can be classified as elements of X with certainty and the set \overline{BX} is the set of elements of U which can possibly be classified as the elements of X employing knowledge B . We can define a measure to express the degree of inexactness of the set X , called roughness measure of X given by

$$\rho(X) = 1 - \frac{|\underline{BX}|}{|\overline{BX}|} \quad (1)$$

for $X \neq \emptyset$, here $|\cdot|$ is the cardinality operator. Obviously $0 \leq \rho(X) \leq 1$, for every B and $X \subseteq U$. If $\rho(X) = 0$, the borderline region of X is empty and the set X is B -definable, i.e., X is crisp or precise with respect to the knowledge B . Otherwise, the set X has some nonempty B -borderline region and is therefore B -undefinable, i.e., X is rough or vague with respect to the knowledge B . Thus Rough set theory approximates a rough or imprecise concept by a pair of exact concepts called the lower and upper approximations.

2.2. Intuitionistic fuzzy set (IFS)

In fuzzy set theory [29], a fuzzy set A in a finite set $X = \{x_1, x_2, \dots, x_n\}$ may be represented mathematically as $A = \{(x, \mu_A(x)) | x \in X\}$

where the function $\mu_A(x) : X \rightarrow [0, 1]$ is the degree of membership of an element $x \in X$ in A . Thus automatically the degree of non-membership is $1 - \mu_A(x)$.

The intuitionistic fuzzy sets suggested by Atanassov [30] are generalization of fuzzy sets whose elements are characterized by a membership, as well as a non-membership value, which give us an additional possibility to represent imperfect knowledge. An intuitionistic fuzzy set A in X is represented mathematically as

$$A = \{(x, \mu_A(x), \nu_A(x), \pi_A(x)) | x \in X\} \quad (2)$$

where the function $\mu_A(x), \nu_A(x) : X \rightarrow [0, 1]$ are the degrees of membership and non-membership of an element x in a finite set X with the necessary condition $0 \leq \mu_A(x), \nu_A(x) \leq 1$. The third parameter $\pi_A(x)$ is known as an intuitionistic fuzzy index or a hesitation degree of $x \in A$. It is obvious that $0 \leq \pi_A(x) \leq 1$ for each x and $\pi_A(x) = 1 - (\mu_A(x) + \nu_A(x))$. The application of intuitionistic fuzzy sets on images gives another degree of freedom to deal with vagueness and uncertainty in image data.

3. Proposed Algorithm

This section describes the flow of complete algorithm for segmentation of brain MR images using rough set based intuitionistic FCM clustering.

3.1. Intuitionistic fuzzy image representation

Intuitionistic fuzzy image is constructed from intuitionistic fuzzy generator (IFG). Intuitionistic fuzzy image representation is used for image segmentation in [22,31,32]. For an image of size $M \times N$ pixels, having intensity levels between 0 to $L - 1$, the IFS representation of the image is given as

$$I = \{x_{ij}, \mu_I(x_{ij}), \nu_I(x_{ij}), \pi_I(x_{ij})\}, \quad 1 < i < M, \quad 1 < j < N \quad (3)$$

where $\mu_I(x_{ij})$, $\nu_I(x_{ij})$ and $\pi_I(x_{ij})$ are the degree of membership, non-membership and hesitancy of the (i, j) th pixel in the image respectively. Membership value at each pixel location is calculated as the normalized intensity level. Normalization gives intensity values in the range of 0–1. These normalized values are used as fuzzy membership values of IFS image representation. We propose a new fuzzy complement function for calculating the non-membership value based on the fact that

there is a high degree of certainty when the membership value is close to 0 or 1 (i.e. less or no hesitation) and the degree of certainty is less when membership value approaches 0.5 (i.e. high degree of hesitation). Intuitionistic fuzzy complement is calculated as

$$N(\mu(x)) = (1 - \mu(x)) \left(\exp\left(\frac{-\mu(x)}{a\sigma}\right) \right)^{1/a} \quad (4)$$

N stands for negation (complement). $N(\mu(x))$ is used to represent intuitionistic fuzzy complement. Multiplication by $(1 - \mu(x))$ ensures that non-membership values always lie between 0 and 1. Here, $N(1) = 0$ and $N(0) = 1$. σ is the standard deviation of membership values $\mu(x)$, which is in the range of 0.37–0.38. The non-membership values are calculated using Eq. (4). Thus, IFS

image becomes $I_a^{IFS} = \{x_{ij}, \mu_I(x_{ij}), \nu_I(x_{ij}), \pi_I(x_{ij})\}$, where $\nu_I(x_{ij}) = (1 - \mu_I(x_{ij})) \left(\exp\left(\frac{-\mu_I(x_{ij})}{a\sigma}\right) \right)^{1/a}$ and $\pi_I(x_{ij}) = 1 - \mu_I(x_{ij}) - \nu_I(x_{ij})$.

Plot of proposed intuitionistic fuzzy index for $a = 1.5$, $a = 5$ and $a = 6$ is shown in Fig. 1(a)–(c) respectively. The plot is symmetric for $a > 1.5$. For $a = 5$, the range of intuitionistic fuzzy index is 0 to less than 0.14, whereas for $a = 6$ the range is very small. Therefore, we used $a = 5$ for our experimentation. This parameter is independent of the patient/scanner.

The performance of proposed intuitionistic fuzzy complement is compared with Sugeno intuitionistic fuzzy complement function $N(\mu(x)) = \frac{(1 - \mu(x))}{(1 + \lambda \mu(x))}$, $-1 < \lambda < \infty$ [26] and Yagers intuitionistic fuzzy complement function $N(\mu(x)) = (1 - \mu(x))^\omega$, $0 < \omega < \infty$ [27]. The plot of Sugeno, Yagers and Proposed intuitionistic fuzzy index are shown in Fig. 2(a)–(c) respectively.

It is observed from Fig. 2 that for membership values close to 0 or 1, the intuitionistic fuzzy index is close to 0 for Sugeno, Yagers and Proposed intuitionistic fuzzy complement index. But for membership value close to 0.5, proposed intuitionistic fuzzy complement gives maximum value of intuitionistic fuzzy index. It can be seen from Fig. 2(a) that the plot of intuitionistic fuzzy index vs membership value is symmetric for the proposed method, whereas it is not symmetric in case of the other two methods.

3.2. Intuitionistic fuzzy roughness measure

The fuzzy histogram and the intuitionistic fuzzy histogram can be correlated with the concept of approximation space in the rough set theory. The histogram value of the $\mu_I(x_{ij})$ th

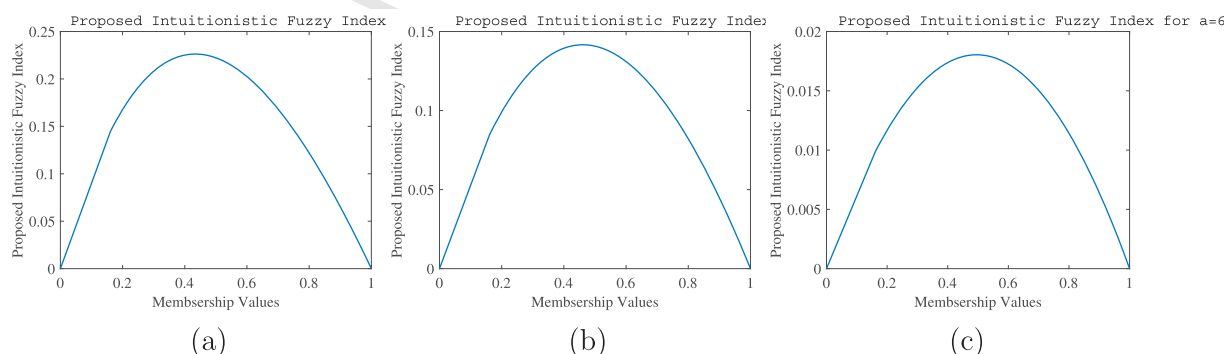


Fig. 1 – Plot of proposed intuitionistic fuzzy index for (a) $a = 1.5$, (b) $a = 5$, and (c) $a = 6$.

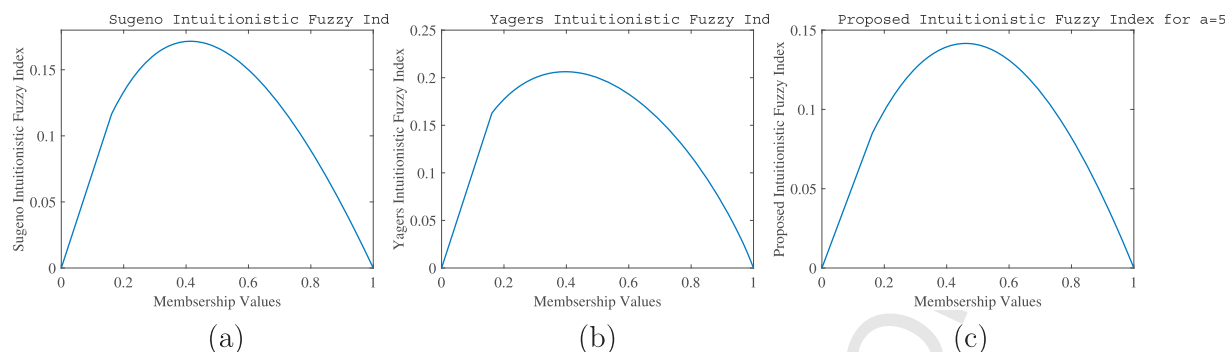


Fig. 2 – (a) Plot of Sugeno intuitionistic fuzzy index for $\lambda = 2$. (b) Plot of Yagers intuitionistic fuzzy index for $\omega = 0.85$. (c) Plot of Proposed intuitionistic fuzzy index for $\alpha = 5$.

membership is the set of pixels which definitely belong to the class of membership and therefore, can be considered as the lower approximation and the intuitionistic fuzzy histogram value of the $\mu_i(x_{ij})$ th membership representing the set of pixel belonging to the similar membership with uncertainty and therefore can be considered as upper approximation. If $f_i(g)$ and $F_i(g)$ are the lower and upper approximation of an image $I(m, n)$, then the intuitionistic fuzzy roughness measure at the g th intensity is given by

$$\rho_i(g) = 1 - \frac{|f_i(g)|}{|F_i(g)|}, \quad 0 \leq g \leq L-1 \quad (5)$$

$|\cdot|$ is the cardinality operator, $f_i(q)$ is the histogram given by

$$f_i(q) = |\mu_l(\mathbf{x}_{ij})|, \quad 0 \leq i \leq M-1, \quad 0 \leq j \leq N-1 \quad (6)$$

and $F_i(q)$ is the intuitionistic fuzzy hston given by

$$F_i(g) = \sum_{m=1}^M \sum_{n=1}^N (1 + \mu(m, n)) \delta(\lfloor 255 * \mu_I(x_{ij}) \rfloor - g), \quad 0 \leq g \leq L-1 \quad (7)$$

here, $\lfloor \cdot \rfloor$ is floor function, $\mu(m, n) = \exp(-\frac{1}{2}(\frac{d_T(m, n)}{\sigma})^2)$ is the Gaussian membership function with σ as the standard deviation of the distance matrix d_T . Gaussian function is used for fuzzy membership because of its smooth variation between the degree of belongingness and non-belongingness. For a $P \times Q$ neighbourhood around a pixel $I(m, n)$, the total distance of all the pixels in the neighbourhood of pixel is then given by

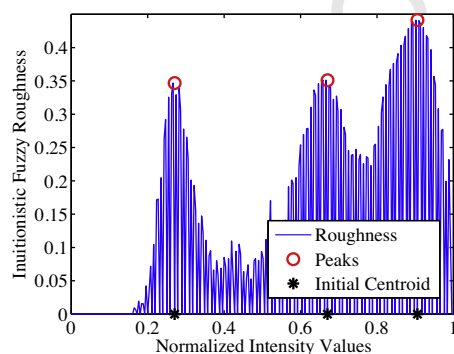


Fig. 3 – Location of initial cluster centroids using intuitionistic fuzzy roughness measure for intuitionistic fuzzy clustering.

$$d_T(m, n) = \sum_{p \in P} \sum_{q \in Q} d(I(m, n), I(p, q)) \quad (8)$$

$d(I(m, n), I(p, q))$ is the Euclidean distance between two pixels $I(m, n)$ and $I(p, q)$ and using intuitionistic fuzzy image representation [33], it is given by

$$d(I(m, n), I(p, q)) = \left\{ \frac{1}{2} ((\mu(I(m, n)) - \mu(I(p, q)))^2) + (v(I(m, n)) - v(I(p, q)))^2 + (\pi(I(m, n)) - \pi(I(p, q)))^2 \right\}^{1/2} \quad (9)$$

The location of peak points of intuitionistic fuzzy roughness measure is used as initial cluster centroids for intuitionistic fuzzy clustering. Initial cluster centroids obtained for brain MR image with 3% noise and 20% intensity homogeneity is shown in Fig. 3.

3.3. Intuitionistic fuzzy clustering

Fuzzy c-means (FCM) is the most effective algorithm for data clustering. FCM was proposed by Dunn [34] and later on it was modified by Bezdek [35]. The standard FCM objective function for partitioning the data $\{x_k\}_{k=1}^N$ into c clusters is given as

$$J_{\text{FCM}}(\mathbf{U}, \mathbf{V}) = \sum_{i=1}^c \sum_{k=1}^N \mu_{ik}^p \|\mathbf{x}_k - \mathbf{v}_i\|^2 \quad (10)$$

where an array $U = \{\mu_{ik}\}$ represents the partition matrix, $V = \{v_i\}_{i=1}^c$ is the prototype of cluster, c is the number of cluster center, N is the number of pixels or data points, x_k is the k th pixel, v_i is the centroid of i th cluster. $\|x_k - v_i\| = d_{ik} = d(x_k, v_i)$ is the distance measure between cluster center v_i and the pixel x_k . μ_{ik} is the fuzzy membership of k th pixel i th cluster. The parameter $p \in (1, \infty)$ is a weighing exponent on each membership (1 for hard clustering and increasing for fuzzy clustering). The partition matrix μ_{ik} and cluster centroid v_i are updated as

$$\mu_{ik} = \frac{1}{\sum_{j=1}^c (d_{ij}^2/d_{ik}^2)^{1/(p-1)}}, \quad v_i = \frac{\sum_{k=1}^N \mu_{ik}^p x_k}{\sum_{k=1}^N \mu_{ik}^p} \quad (11)$$

The drawback of FCM for image segmentation is that its objective function does not take into consideration any spatial dependence among pixels of image. Secondly, the

membership function of FCM is mostly decided by $d(x_k, v_i)$, which measures the similarity between the pixel intensity and the cluster center. Higher membership depends on closer intensity values to the cluster center. Hence membership function is highly sensitive to noise. In MR image with noise and intensity inhomogeneity, the performance of FCM methods decreases and results in improper segmentation.

To deal with these problems we have used Euclidean distance based on intuitionistic fuzzy set [33] which is given by

$$d_{IFS}(x_k, v_i) = \left\{ \frac{1}{2} ((\mu(x_k) - \mu(v_i))^2 + (v(x_k) - v(v_i))^2 + (\pi(x_k) - \pi(v_i))^2) \right\}^{1/2} \quad (12)$$

Using this intuitionistic fuzzy distance measure, partition matrix and cluster centroid are updated as

$$\mu_{ik(IFS)} = \frac{1}{\sum_{j=1}^c \left(\frac{d_{IFS}(x_k, v_i)}{d_{IFS}(x_k, v_j)} \right)^{2/(p-1)}} \quad (13)$$

$$v_{i(IFS)} = \frac{\sum_{k=1}^N \mu_{ik(IFS)}^p \mu(x_k)}{\sum_{k=1}^N \mu_{ik(IFS)}^p} \quad (14)$$

While updating membership function, membership, non-membership and hesitation of pixel value are considered. This compensates for the intensity inhomogeneity and noise in brain MR images and results in more appropriate tissue segmentation.

4. Experimental results

4.1. Real images

The proposed algorithm is applied on real images from NKP Salve Institute of Medical Science and Lata Mangeshkar Hospital, Nagpur. The algorithm is tested on total 24 real brain images with tumor type Oligo and High Grade Glioma. Comparison of segmentation results obtained by proposed method, BCFCM [4] and IFS clustering [24] for four images are shown in Fig. 4. First row shows the original real brain images. The images in the second, third and fourth row are results of BCFCM [4], IFS clustering [24] and proposed RIFCM method respectively. The results of segmentation on real brain images using proposed algorithm are validated by Radiologist. Since the ground truth data was not available, the quantitative validation was not possible. We asked three Radiologists of renowned Hospitals independently and then qualitative validation of segmentation results was carried out which is quite consistent with expert Radiologists evaluation.

First image is T2 weighted flair image with tumor type Oligo, which is in the frontal region on the right side and anterior, medial and posterior. The segmentation using proposed method is picking up the tumor tissue. It has rightly excluded the necrotic portion of the tumor, cystic component and edema. Whereas in the results obtained by IFS clustering and BCFCM, segmentation has excluded the cystic component but is picking up necrotic portion and edema. Second image in

the first row shows another T2 flair image with tumor type Oligo. Here segmentation by the proposed method has rightly excluded cystic component and edema portion and segmented only tumor. Whereas, in the result obtained by IFS clustering method, the segmentation is picking up the tumor tissue, cystic component of the tumor as well as the skull portion. BCFCM method has rightly excluded edema portion, but segmentation is picking up cystic component and skull portion.

Third image of first row shows T2 flair image with tumor High Grade Glioma. It is observed, that segmentation by proposed method has rightly excluded edema portion and segmented tumor properly. In the results obtained by IFS clustering and BCFCM, segmentation is picking up CSF, edema and skull portion and have rightly excluded tumor region. Fourth image of first row shows another T2 flair image with tumor type High Grade Glioma. Here segmentation by the proposed method has rightly excluded edema portion and segmented only tumor. Whereas, in the result obtained by BCFCM and IFS clustering method, the segmentation is picking up the tumor tissue, edema portion as well as skull portion.

Fig. 5(a) shows T2 weighted flair image with tumor type Oligo. The segmentation using proposed method has separated the tumor tissue (red color) from cystic component (green color) and edema (blue) as shown in Fig. 5(a). Fig. 5(c) shows another T2 flair image with tumor type Oligo. Here segmentation by the proposed method has rightly excluded cystic component (green color) and edema portion (blue color) and segmented only tumor (red color) as depicted in Fig. 5(d).

Fig. 6(a) shows T2 flair image with tumor High Grade Glioma. It is observed, that segmentation by proposed method shown in Fig. 6(b) has rightly excluded cystic component (green color) and segmented tumor properly (red color). Fig. 6(c) shows another T2 flair image with tumor type High Grade Glioma. Here segmentation by the proposed method has rightly excluded edema portion (blue color) and segmented only tumor (red color) as depicted in Fig. 6(d).

4.2. Synthetic images

The proposed method is applied on simulated brain MR images from BrainWeb: Simulated Brain Database [36]. Each image is provided with anatomical ground truth which provides tissue class. We have used 2D transverse slices (Slices No. 91, 95 and 98), T1-weighted images with 1 mm resolution at different intensity inhomogeneity (0%, 20% and 40%) and at different noise level (0%, 1%, and 3%) for the segmentation. Fig. 7 shows the results of rough set based intuitionistic fuzzy clustering (RIFCM) algorithm on brain MR image with 3% noise and 20% intensity inhomogeneity. In Fig. 7, first row shows the original image, corresponding ground truth of brain tissues and segmentation result. Three intuitionistic fuzzy set (IFS) regions for each of CSF, GM and WM are shown in second row and segmented region of CSF, GM and WM are depicted in third row. From ground truth and segmentation result, it is observed that tissue segmentation obtained by applying proposed method is consistent with the ground truth.

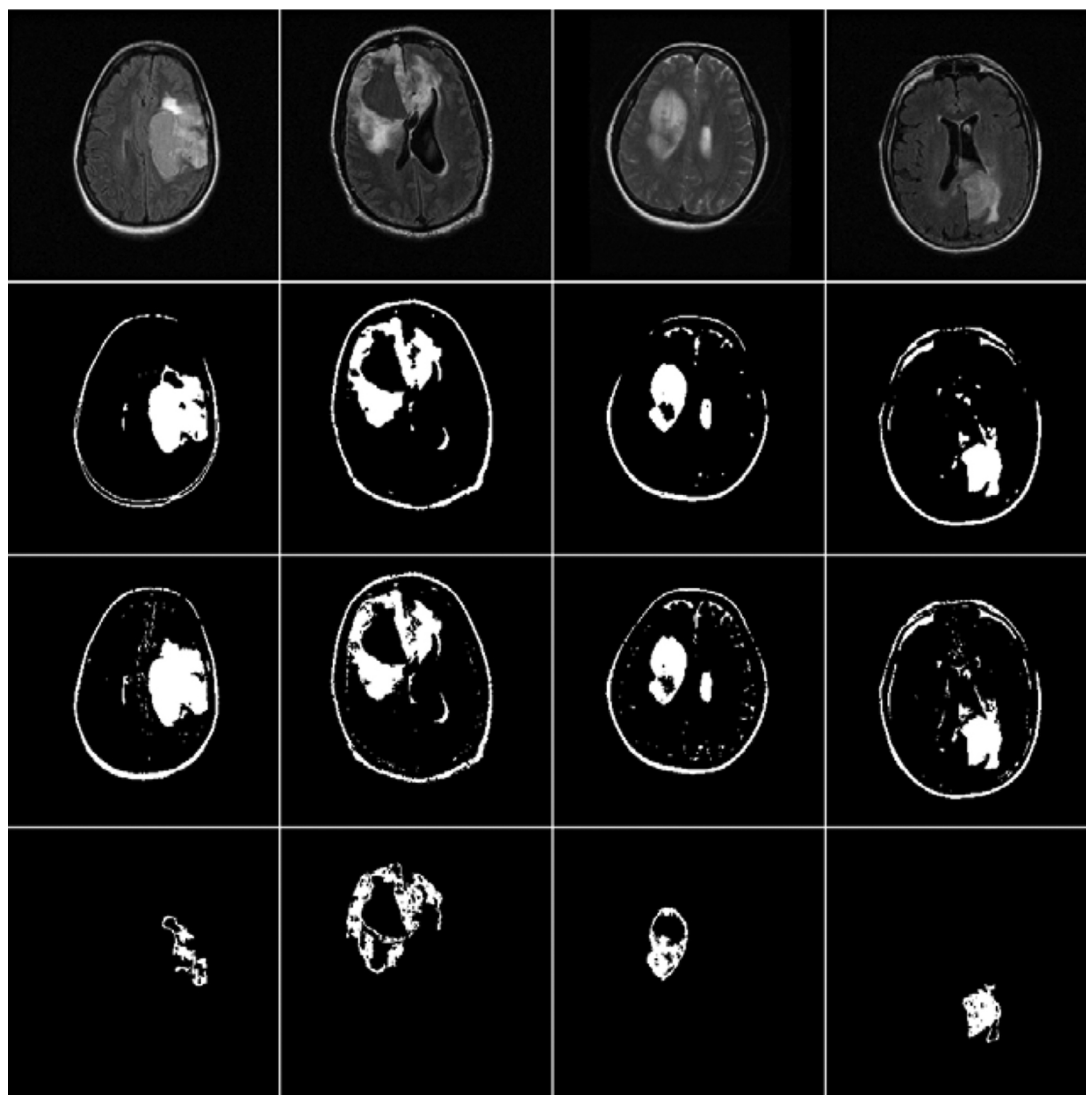


Fig. 4 – Comparison of segmentation results on real brain images. First row shows the original brain images. The images in the second, third and fourth row are results of BCFCM, IFS clustering and proposed RIFCM algorithm respectively.

4.3. Quantitative evaluation

To validate the performance of proposed algorithm, quantitative evaluation is carried using following indices.

Jaccard Similarity (JS) [37] is defined as the ratio between intersection and union of two sets representing the obtained segmentations and ground truth and is given by

$$JS(S_1, S_2) = \frac{|S_1 \cap S_2|}{|S_1 \cup S_2|} \quad (15)$$

Dice Coefficient (DC)/Overlap Ratio [37] is the set of agreement between the segmentation result and the ground truth. It is as defined as

$$DC(S_1, S_2) = \frac{2|S_1 \cap S_2|}{|S_1| + |S_2|} \quad (16)$$

JS values are more sensitive when sets are very similar and DC values give relative index of overlap between obtained segmentation and ground truth. S_1 and S_2 are the numbers of the

pixels classified as one class using proposed algorithm and the ground truth, respectively. $|S_1 \cap S_2|$ are the number of pixels segmented as one class in both results. $|S_1 \cup S_2|$ are the number of pixels common to both results. These measure attains a value of 100% when segmentation results matches completely with the ground truth and is 0% when there is no match.

Confusion Table [9], a matrix that gives False Positives (FP), False Negatives (FN) and True Positives (TP) of brain tissues for a particular class on rows over the class of the ground truth on columns. Therefore, the diagonal entry of this confusion table represents the true positives (TP) for each class. The False Negative (FN) is defined as the percentage of the pixels of the ground truth mistakenly segmented as the other classes. The False Positive (FP) is computed as the percentage of the pixels incorrectly segmented as the class over the pixels that do not belong to the class in the ground truth.

Based on True Negatives (TN), False Positives (FP), False Negatives (FN), and True Positives (TP), three more evaluation

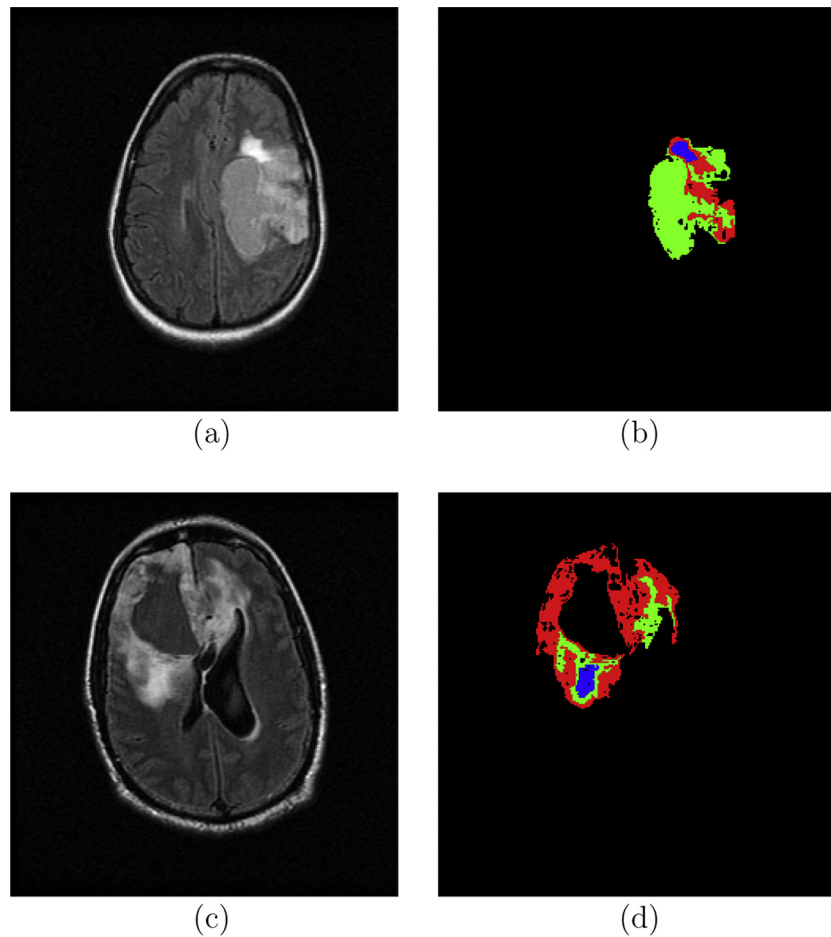


Fig. 5 – Results of segmentation on real images using proposed method. (a) T2 flair image with tumor type Oligo. (b) Edema, cystic component and tumor are shown in blue, green and red color respectively. (c) T2 flair image with tumor type Oligo. (d) Edema, cystic component and tumor are shown in blue, green and red color respectively as validated by Radiologist. (For interpretation of the references to color in this figure legend, the reader is referred to the web version of the article.)

parameters are also used for comparisons which are defined as follows [6].

1. Under segmentation (percentages of negative false segmentation) given by $UnS = FP/TN$.
2. Over segmentation (percentage of positive false segmentation) given by $OvS = FN/TP$.
3. Incorrect segmentation (percentage of total false segmentation) give by $InS = (FP + FN)/N$.

The results of proposed algorithm are compared with modified fast FCM algorithm (MFCM) [38] on the basis of Jaccard Similarity (JS) and Dice Coefficient (DC). Table 1 shows the Jaccard Similarity (JS) and Dice Coefficient (DC) for segmented region of CSF, GM and WM obtained for T1-weighted MR brain images (slice No. 91) with 0% intensity inhomogeneity and varying noise level as 1%, 5%, 9% and 13%. It is observed from Table 1, that JS and DC values for CSF and GM using proposed method is higher than MFCM method [38] for all the images with noise level of 1%, 5%, 9% and 13%.

The proposed algorithm is also compared with nonlocal fuzzy segmentation (NLFCM) method [39]. The results are evaluated on the basis of overlap ratio (DC value). Fig. 8 shows the comparison of overlap ratios for brain MR images with 0% and 20% intensity inhomogeneity and varying noise level from 0% to 9%.

It is observed from Fig. 8, that for the brain MR images with 20% intensity inhomogeneity and varying noise level, overlap ratios obtained for GM using proposed method are higher than those obtained by nonlocal FCM (NLFCM) method. And for 3% noise level, overlap ratios obtained for WM using proposed method are higher than those obtained by nonlocal FCM (NLFCM).

The results RIFCM segmentation on brain MR images (slice no.95) for 0% intensity inhomogeneity and varying noise levels as 1%, 3%, 5%, 7% and 9% are compared to the Rough c-means (RCM) [40], Rough fuzzy means (RFCM) [41], Shadowed c-means (SCM) [42], Rough possibilistic fuzzy c-means (RPFCM) [43] and Generalized rough FCM (GRFCM) [44] algorithms. The accuracy of all six algorithms in segmenting GM and WM of brain MR images with 0%

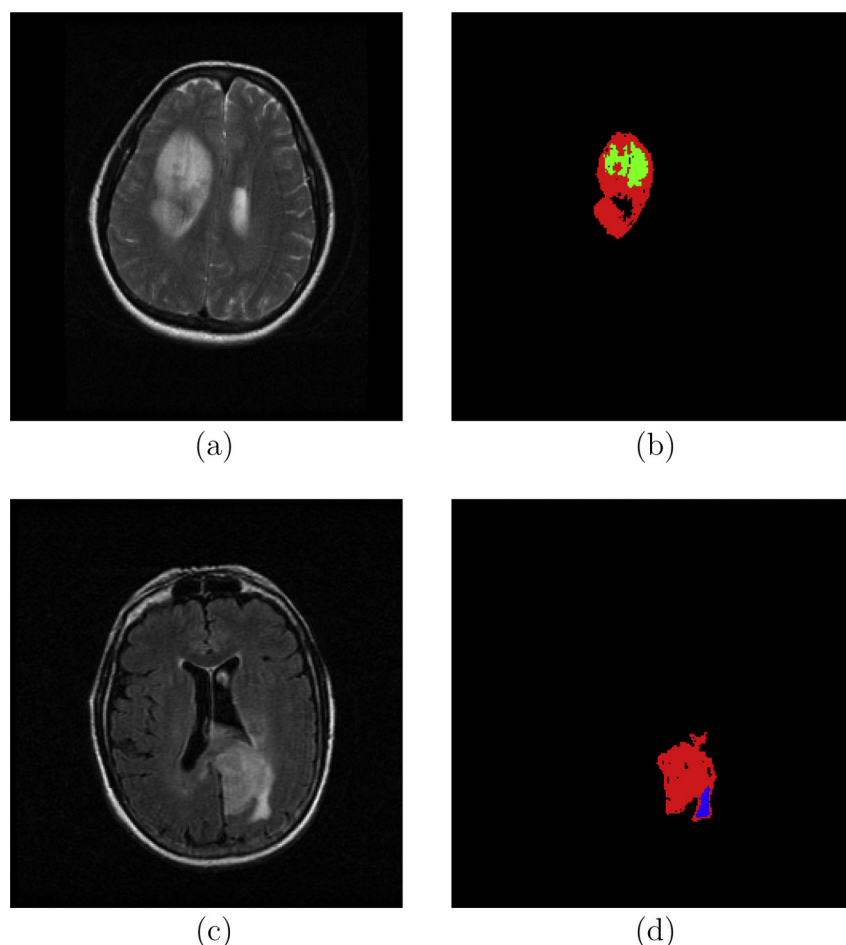


Fig. 6 – Results of segmentation on real images using proposed method. (a) T2 flair image with tumor High Grade Glioma. (b) Cystic component and tumor are shown in green and red respectively. (c) T2 flair image with tumor High Grade Glioma. (d) Edema and tumor are shown in blue and red respectively as validated by Radiologist. (For interpretation of the references to color in this figure legend, the reader is referred to the web version of the article.)

intensity inhomogeneity and noise level varying as 1%, 3%, 5%, 7% and 9% compared on the basis of DC value is shown in Fig. 9. This comparison demonstrates that the proposed algorithm produce the most accuracy segmentation and has the best ability to denoise.

It is observed from Fig. 9, that for the brain MR images with 0% and 20% intensity inhomogeneity and varying noise level, overlap ratios obtained for GM using proposed method are higher than those obtained by nonlocal FCM (NLFCM) method. And for 3% noise level, overlap ratios obtained for WM using proposed method are higher than those obtained by nonlocal FCM (NLFCM).

RIFCM segmentation results are also compared with interval-valued possibilistic fuzzy c-means clustering algorithm (IPFCM) [45] on the basis of Kappa Index overlap measure $KI = \frac{2 \cdot TP}{2 \cdot TP + FN + FP}$ and Recognition Rate (RR) [45]. RR is the percentage of correctly recognized data in the whole data set. The results of comparison on brain MR images with 0% intensity inhomogeneity and varying noise level as 0%, 3%, 5%, 7% and 9% are shown in Table 2. It is observed from Table 2 that for heavy noise above 3%, RIFCM outperforms IPFCM in both the index.

Results of segmentation by proposed algorithm are also compared with segmentation results using BCFCM [4] and IFS clustering [24] method and qualitative and quantitative analysis is carried out. The segmentation results for brain MR images with 20% intensity inhomogeneity and varying noise level from 0% to 3% BCFCM, IFS clustering and proposed RIFCM algorithm are shown in Fig. 10.

The images in the first row show the brain MR images with 20% intensity inhomogeneity and varying noise level as 0%, 1% and 3%. The images in the second row are the results of BCFCM, images in the third row are the results of IFS clustering and the images in the fourth row are the results of proposed RIFCM method. It is observed from Fig. 10, that as the noise level is increased from 0% to 3%, there is overlap of pixel intensities in gray matter and white matter with the results obtained with BCFCM and IFS clustering. Whereas with proposed method, for the noise level from 0% to 3%, distinction between the boundaries of gray matter and white matter is clearly seen (Fig. 10).

The segmentation results are also evaluated on the basis of confusion table. **Table 3** shows the confusion table for the image with 3% noise and at intensity inhomogeneity of 20%.

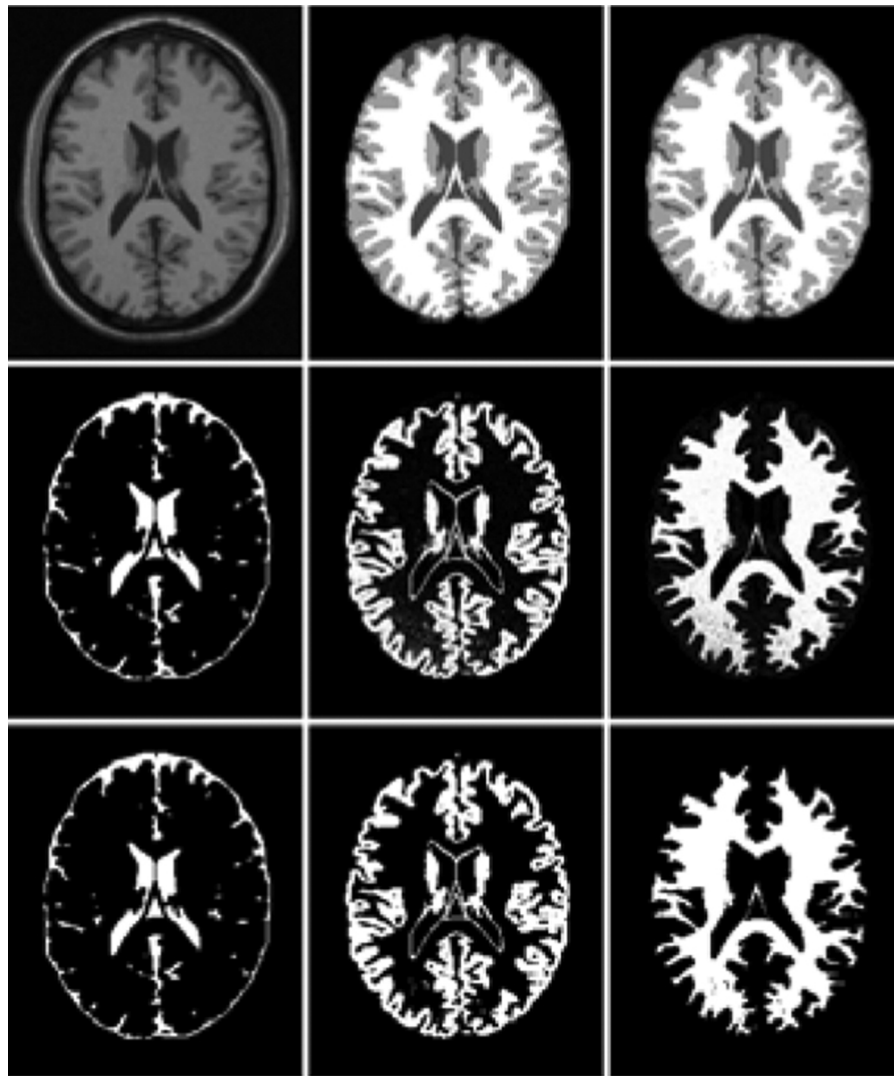


Fig. 7 – First row: Brain MR image with 3% noise and 20% intensity inhomogeneity, ground truth and segmentation result by proposed algorithm. Second row: IFS rough region of CSF, GM and WM. Row 3: Region of CSF, GM and WM.

Table 1 – Comparison of Jaccard Similarity (JS) and Dice coefficient (DC) for brain MR images with 0% intensity inhomogeneity and varying noise level as 1%, 5%, 9% and 13% using proposed RIFCM and MFCM [38] method.

Noise level	Tissue class	Jaccard Similarity		Dice Coefficient	
		MFCM	RIFCM	MFCM	RIFCM
1%	CSF	0.8853	0.8992	0.9391	0.9469
	GM	0.9218	0.9703	0.9593	0.9849
	WM	0.9676	0.9564	0.9835	0.9777
5%	CSF	0.8583	0.9116	0.9236	0.9537
	GM	0.8885	0.9565	0.941	0.9777
	WM	0.9467	0.9456	0.9726	0.9720
9%	CSF	0.8128	0.9016	0.8964	0.9482
	GM	0.8463	0.9257	0.9168	0.9614
	WM	0.9212	0.9219	0.9648	0.9593
13%	CSF	0.7118	0.7968	0.8351	0.8869
	GM	0.7002	0.8019	0.8236	0.8900
	WM	0.8326	0.7755	0.9106	0.8735

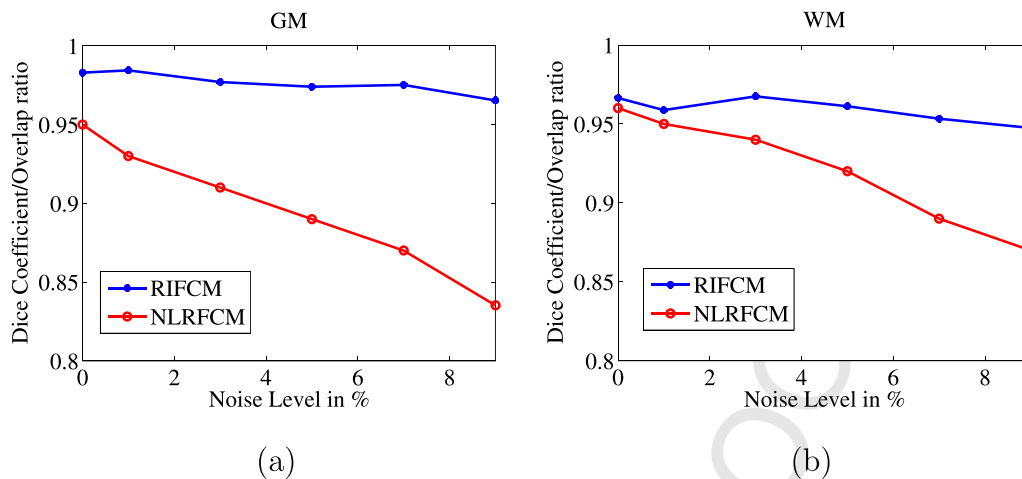


Fig. 8 – Comparison of DC value/overlap ratios obtained using proposed RIFCM method and NLRFCM for (a) GM and (b) WM for brain MR images with 20% intensity inhomogeneity varying noise level from 0% to 9%.

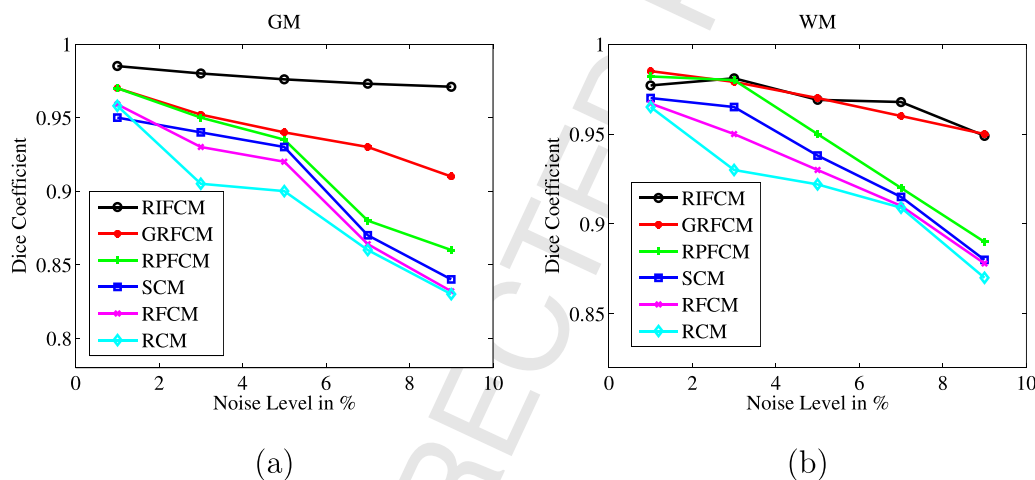


Fig. 9 – Comparison of DC values of GM (left) and WM (right) obtained by applying six algorithms for brain MR image with 0% Intensity inhomogeneity varying noise level from 0% to 9%.

Table 2 – Comparison RR and KI obtained using IPFCM and RIFCM.

Noise level	Evaluation index	IPFCM	RIFCM
0%	RR	0.9893	0.9799
	KI	0.9915	0.9947
3%	RR	0.9753	0.9711
	KI	0.9835	0.9877
5%	RR	0.9578	0.9602
	KI	0.9677	0.9795
7%	RR	0.9346	0.9443
	KI	0.9499	0.9645
9%	RR	0.9022	0.9215
	KI	0.9252	0.9445

It is observed from Table 3, True positive values of CSF and WM for brain MR image with 3% noise and 20% intensity inhomogeneity using IFS clustering (86.39 and 80.62) and BCFCM method (75.23 and 76.25) without automatic initialization of centroid is much lower the values obtained by proposed method (95.85 and 94.23).

To demonstrate the superiority of proposed fuzzy complement function, we have compared the performance of experimental results obtained by proposed function with the results obtained by Sugeno intuitionistic fuzzy complement function $N(\mu(x)) = \frac{(1-\mu(x))}{(1+\lambda\mu(x))}$, $-1 < \lambda < \infty$ [26] and Yagers intuitionistic fuzzy complement function $N(\mu(x)) = (1-\mu(x)^\omega)^{1/\omega}$, $0 < \omega < \infty$ [27].

The value of $\lambda = 2$ and $\omega = 0.85$ are selected from reference [23,24]. Experimentally it is found that with $\lambda \leq 1$ and $\lambda \geq 5$, segmentation accuracy of gray matter (GM) is reduced to 93% from 98%. So, to obtain better image result, $\lambda = 2$ is used. Similarly, with $\lambda \leq 1$ and $\lambda \geq 5$, segmentation accuracy of

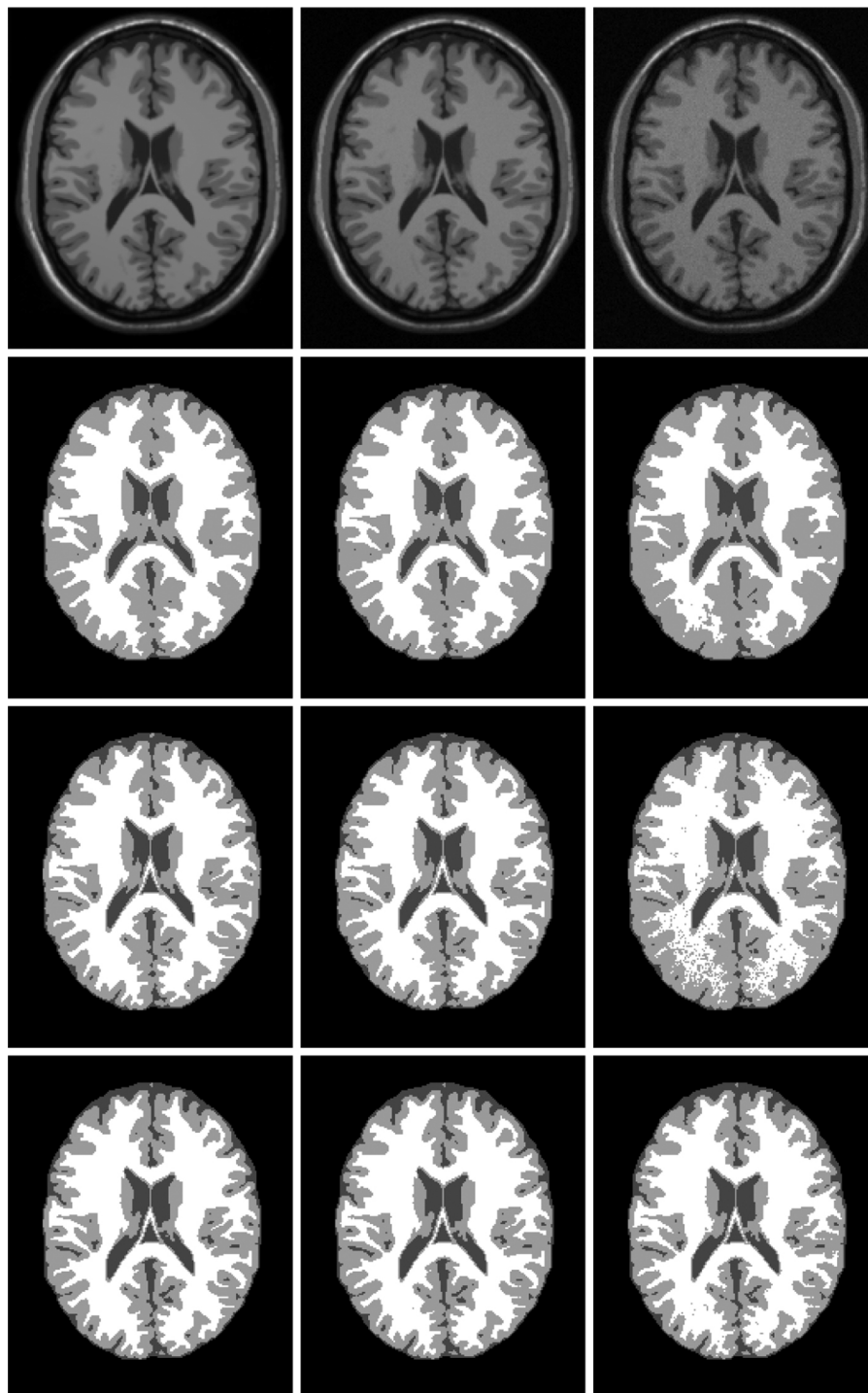


Fig. 10 – Segmentations of brain MR images for 20% intensity inhomogeneity and varying noise level from 0% to 3%. First row show the original brain MR images. The images in the second, third and fourth row are results of BCFCM, IFS clustering and RIFCM respectively.

White Matter (WM) is reduced to 92% from 94%. So, to obtain better segmentation result, $\omega = 0.85$ is used.

Table 4 shows the confusion table for images with 3% noise and 20% intensity inhomogeneity using proposed fuzzy complement compared to Sugeno and Yagers fuzzy

complement function. From Table 4, it is observed that true positive for CSF (95.17 ± 1.61) and WM (94.45 ± 2.07) using proposed fuzzy complement is higher compared to those obtained with Yagers fuzzy complement function for CSF (94.77 ± 0.26) and WM (94.04 ± 0.87) and with Sugeno fuzzy

Table 3 – Confusion table for images with 3% noise and 20% intensity inhomogeneity.

Classified pixels	Ground truth			
	CSF	GM	WM	FP
Proposed RIFCM method				
CSF	95.85	0.85	0	2.08
GM	4.14	98.19	5.77	1.7
WM	0	0.94	94.23	0.7
FN	4.14	1.8	5.77	
IFS Clustering method				
CSF	86.39	0.02	0	0.06
GM	13.6	99.9	19.37	5.58
WM	0	0	80.62	0
FN	13.6	0.02	19.37	
BCFCM method				
CSF	75.23	0.42	0	1.02
GM	24.76	99.57	23.74	10.17
WM	0	0	76.25	0.7
FN	24.7	0.42	23.74	

complement function for CSF (93.28 ± 0.61) and WM (93.58 ± 1.64). For GM, true positive value using propose fuzzy complement is 98.45 ± 0.1 , which is slightly lower than those obtained by Sugeno Fuzzy Complement (98.73 ± 0.25), but higher than the value obtained by Yagers fuzzy complement (98.45 ± 0.1).

Table 5 shows UnS, OvS and InS for brain MR image with 3% noise and 20% intensity inhomogeneity using proposed hesitation index, Sugeno fuzzy complement and Yagers fuzzy complement.

Average values of UnS, OvS and InS obtained for brain image with 3% noise and 20% intensity inhomogeneity using proposed fuzzy complement function (0.25 ± 0.04 , 4.28 ± 0.31 and 0.88 ± 0.01) is lower than those obtained with Sugeno fuzzy complement (0.27 ± 0.05 , 5.46 ± 0.44 and 1.01 ± 0.06) and Yagers complement (0.26 ± 0.02 , 4.47 ± 0.36 and 0.9 ± 0.04).

Table 4 – Confusion table for images with 3% noise and 20% intensity inhomogeneity.

	Ground truth			
	CSF	GM	WM	FP
Proposed Fuzzy Complement				
Classified Pixels				
CSF	95.17 ± 1.61	0.86 ± 0.22	0	2.14 ± 0.41
GM	4.82 ± 1.61	98.7 ± 0.1	5.54 ± 0.76	1.89 ± 0.48
WM	0	0.96 ± 0.17	94.45 ± 0.76	0.71 ± 0.15
FN	4.82 ± 1.61	1.82 ± 0.1	5.54 ± 0.76	
Yagers Fuzzy Complement				
Classified Pixels				
CSF	94.77 ± 0.26	0.66 ± 0.25	0	1.69 ± 0.78
GM	5.225 ± 0.26	98.45 ± 0.1	5.95 ± 0.87	2.08 ± 0.13
WM	0	0.88 ± 0.34	94.04 ± 0.87	0.65 ± 0.24
FN	5.22 ± 0.26	1.54 ± 0.1	5.95 ± 0.87	
Sugeno Fuzzy Complement				
Classified Pixels				
CSF	93.28 ± 0.61	0.44 ± 0.19	0	1.13 ± 0.58
GM	6.71 ± 0.61	98.73 ± 0.25	6.41 ± 1.64	2.69 ± 0.36
WM	0	0.81 ± 0.45	93.58 ± 1.64	0.6 ± 0.32
FN	6.71 ± 0.61	1.26 ± 0.25	6.41 ± 1.64	

Table 5 – Under segmentation (UnS), Over segmentation (OvS) and Incorrect segmentation (InS) for brain MR image with 3% noise and 20% intensity inhomogeneity.

Tissue class	Evaluation parameter in %	Sugeno	Yagers	Proposed
CSF	UnS	0.1 ± 0.04	0.13 ± 0.05	0.15 ± 0.04
	OvS	7.41 ± 0.46	5.52 ± 0.3	5.09 ± 1.8
	InS	0.56 ± 0.02	0.49 ± 0.03	0.49 ± 0.05
GM	UnS	0.57 ± 0.07	0.45 ± 0.02	0.41 ± 0.11
	OvS	1.14 ± 0.28	1.57 ± 0.11	1.86 ± 0.05
	InS	0.66 ± 0.11	0.64 ± 0.03	0.66 ± 0.08
WM	UnS	0.14 ± 0.11	0.2 ± 0.08	0.22 ± 0.04
	OvS	7.84 ± 2.05	6.34 ± 0.99	5.87 ± 0.86
	InS	1.8 ± 0.31	1.57 ± 0.12	1.49 ± 0.17
Average	UnS	0.27 ± 0.05	0.26 ± 0.02	0.25 ± 0.04
	OvS	5.46 ± 0.44	4.47 ± 0.36	4.28 ± 0.31
	InS	1.01 ± 0.06	0.9 ± 0.04	0.88 ± 0.01

5. Conclusion

A rough set based intuitionistic fuzzy c-means clustering algorithm is presented for segmentation of MR images corrupted by intensity inhomogeneities and noise. We proposed a new automated method to determine initial values of centroids using intuitionistic fuzzy roughness index. To address intensity inhomogeneities and noise in brain MR images, intuitionistic fuzzy image representation using proposed intuitionistic fuzzy complement function is used. We have compared the performance of proposed method with IFS clustering and BCFCM algorithm for real and synthetic images and also with other rough set based FCM clustering algorithms. We have also compared the performance of proposed fuzzy complement function with Sugeno and Yagers fuzzy complement. Our results show that the proposed algorithm is more robust to intensity inhomogeneity and noise, and hence can produce accurate brain MR image segmentation.

Acknowledgements

The authors would like to thank Dr. R.V. Phadke, Prof. and Head, Department of Radiology, Sanjay Gandhi Post Graduate Institute of Medical Sciences, Lucknow, for help in interpretation of brain MR images and validation of results.

REFERENCES

- [1] Pham DL, Prince JL. An adaptive fuzzy c-means algorithm for image segmentation in presence of intensity inhomogeneity. *Pattern Recognit Lett* 1999;20(1):57–68.
- [2] Liew AWC, Leung S, Lau W. Fuzzy image clustering incorporating spatial continuity. *Inst Elect Eng Vis Image Signal Process* 2000;147:185–92.
- [3] Li L, Li X, Wei X, Liang Z. A unifying framework for inhomogeneity correction and partial volume segmentation of brain MR image. *IEEE Nuclear Science Symposium Conference Record*; 2004.
- [4] Ahmed MN, Yamany S, Mohamed N, Farag A, Moriarty T. A modified fuzzy c-means algorithm for bias field estimation and segmentation of MRI data. *IEEE Trans Med Imaging* 2002;21(3):193–9.
- [5] Chen S, Zhang D. Robust image segmentation using FCM with spatial constraint based on new kernel-induced distance measure. *IEEE Trans Syst Man Cybern B* 2004;34(4):1907–16.
- [6] Shen S, Sandham WA, Granat MH, Sterr A. Mri fuzzy segmentation of brain tissue using neighborhood attraction with neural-network optimization. *IEEE Trans Inf Technol Biomed* 2005;9(3).
- [7] Cai W, Chen S, Zhang D. Fast and robust fuzzy c-means clustering algorithms incorporating local information for image segmentation. *Pattern Recognit* 2007;40:825–38.
- [8] Yang MS, Tsai HS. A gaussian kernel-based fuzzy c-means algorithm with a spatial bias correction. *Pattern Recognit Lett* 2008;29:1713–25.
- [9] Wang H, Fei B. A modified fuzzy c-means classification method using a multiscale diffusion filtering scheme. *Med Image Anal* 2009;13:193–202.
- [10] Zavaljevski A, Dhawan A, Gaskil M, Ball W, Johnson J. Multi-level adaptive segmentation of multi-parameter MR brain images. *Comput Med Imaging Graph* 2000;24(2):87–98.
- [11] Corso JJ, Sharon E, Dube S, El-Saden S, Sinha U, Yuille A. Efficient multilevel brain tumor segmentation with integrated bayesian model classification. *IEEE Trans Med Imaging* 2008;27:629–40.
- [12] Bricq S, Collet C, Armspach J. Unifying framework for multimodal brain MRI segmentation based on Hidden Markov Chains. *Med Image Anal* 2008;12:639–52.
- [13] Adelino R, da Silva F. Bayesian mixture models of variable dimension for image segmentation. *Comput Methods Progr Biomed* 2009;94:1–14.
- [14] Huang A, Abugharbieh R. A hybrid geometricstatistical deformable model for automated 3-D segmentation in brain MRI. *IEEE Trans Biomed Eng* 2009;56(7).
- [15] Scherrer B, Forbes F, Garbay C, Dojat M. Distributed local MRF models for tissue and structure brain segmentation. *IEEE Trans Med Imaging* 2009;28:1278–95.
- [16] Nie J, Xue Z, Liu T, Young GS, Setayesh K, Wong LGSTC. Automated brain tumor segmentation using spatial accuracy-weighted hidden Markov random field. *Comput Med Imaging Graph* 2009;33:431–41.
- [17] Li C, Huang R, Ding Z, Gatenby JC, Metaxas DN, Gore JC. A level set method for image segmentation in the presence of intensity inhomogeneities with application to MRI. *IEEE Trans Med Imaging* 2011;20(7):2007–16.
- [18] Thapaliyaa K, Pyuna JY, Parkb CS, Kwona GR. Level set method with automatic selective local statistics for brain tumor segmentation in MR images. *Comput Med Imaging Graph* 2013;37(7–8):522–37.
- [19] Mohabey A, Ray AK. Fusion of rough set theoretic approximations and FCM for color image segmentation. In: *IEEE Int. Conf. Systems, Man, and Cybernetics*. 2000. pp. 1529–34.
- [20] Mushrif MM, Ray AK. Color image segmentation: rough-set theoretic approach. *Pattern Recognit Lett* 2008;29:483–93.
- [21] Yue XD, Miao DQ, Zhang N, Cao LB, Wu Q. Multiscale roughness measure for color image segmentaion. *Inf Sci* 2012;216:93–112.
- [22] Mushrif MM, Ray AK. A-IFS histon based multithresholding algorithm for color image segmentation. *IEEE Signal Process Lett* 2009;16(3).
- [23] Chaira T, Anand S. A novel intuitionistic fuzzy approach for tumour/hemorrhage detection in medical images. *JSIR* 2011;7:427–34.
- [24] Chaira T. A novel intuitionistic fuzzy c means clustering algorithm and its application to medical images. *Appl Soft Comput* 2011;11:1711–7.
- [25] Dubey YK, Mushrif MM. Segmentation of brain MR images using intuitionistic fuzzy clustering algorithm. *ICVGIP. IIT Bombay, ACM*; 2012978-1-4503-1660-6.
- [26] Sugeno S. Fuzzy measures and fuzzy integrals: a survey. In: Gupta M, Sardis GN, Gaines BR, editors. *Automata and decision process*. Amsterdam/New York: North Holland; 1977. p. 82–102.
- [27] Yager RR. On the measure of fuzziness and negation. Part II. *Inf Control* 1977;44:236–60.
- [28] Pawlak Z. Rough set theory and its applications. *Int J Comput Inf Sci* 1982;11:341–56.
- [29] Zadeh LA. Fuzzy sets. *Inf Control* 1965;8(3):338–53.
- [30] Atanassov KT. Intuitionistic fuzzy sets. *Fuzzy Sets Syst* 1986;20(1):87–96.
- [31] Chaira T, Ray AK. A new measure using intuitionistic fuzzy set theory and its application to edge detection. *Appl Soft Comput* 2008;8(2):919–27.

- [32] Mookiah MR, Acharya UR, Chua CK, Min LC, Ng EY, Mushrif MM, et al. Automated detection of optic disk in retinal fundus images using intuitionistic fuzzy histogram segmentation. *J Eng Med* 2013;227(1):37–49.
- [33] Szmiedt E, Kacprzyk J. Distances between intuitionistic fuzzy sets. *Fuzzy Sets Syst* 2000;114(3):505–18.
- [34] Dunn J. A fuzzy relative of the ISODATA process and its use in detecting compact well separated clusters. *J Cybern* 1974;3(3):32–57.
- [35] Bezdek J. A convergence theorem for fuzzy ISODATA clustering algorithms. *IEEE Trans Pattern Anal Mach Intell* 1980;2:1–8.
- [36] <http://www.bic.mni.mcgill.ca/brainweb/> [accessed January 2012].
- [37] Vovk U, Pernus F, Likar B. A review of methods for correction of intensity inhomogeneity in MRI. *IEEE Trans Med Imaging* 2007;26(3):405–15.
- [38] Ji ZX, Quan-SenSun, Xia DS. A framework with modified fast FCM for brain MR images segmentation. *Pattern Recognit* 2011;44:999–1013.
- [39] Caldaïrou B, Passat N, Habas PA, Studholme C, Rousseau F. A non-local fuzzy segmentation method: application to brain MRI. *Pattern Recognit* 2011;44:1916–27.
- [40] Lingras P, West C. Interval set clustering of web users with rough k-means. *Tech. Rep.*. Halifax, NS, Canada: St. Marys Univ; 2002.
- [41] Maji P, Pal S. Rfcmm: a hybrid clustering algorithm using rough and fuzzy sets. *Fundam Inform* 2007;79:1–22.
- [42] Mitra S, Pedrycz W, Barman B. Shadowed c-means: integrating fuzzy and rough clustering. *Pattern Recognit* 2010;43:1282–91.
- [43] Maji P, Pal SK. Rough set based generalized fuzzy C-means algorithm and quantitative indices. *IEEE Trans Syst Man Cybern B Cybern* 2007;37(6):1529–40.
- [44] Ji ZX, Quan-SenSun, Xia DS. Generalized rough fuzzy c-means algorithm for brain MR image segmentation. *Comput Methods Progr Biomed* 2012;108:644–55.
- [45] Ji Z, Xia Y, Sun Q, Cao G. Interval-valued possibilistic fuzzy c-means clustering algorithm. *Fuzzy Sets Syst* 2014;253:138–56.